Exponentially Loaded Column Gas Chromatography

Thomas Bunting[1] **and Clifton E. Meloan**

Department of Chemistry, Kansas State University, Manhattan, Kan. 66502

Columns possessing an exponential gradient in *k* have been treated theoretically from the viewpoints of solute retention, column efficiency, and resolution. The derived equations have been experimentally verified using a column which closely approximates an exponential gradient—a 25-stage stepwise gradient column.

VARIOUS CHROMATOGRAPHIC PROCEDURES involving the systemic variation of a critical parameter have been developed. Programmed temperature gas chromatography allows for the analysis of widely boiling mixtures in a minimum of time while retaining maximum resolution. Programmed pressure gas chromatography offers the same advantages as programmed temperature gas chromatography and, in addition, is suitable for thermally unstable components and for columns with low maximum substrate operating temperatures. Gradient elution liquid chromatography (*1*) has offered similar advantages to column chromatography.

Purnell (*2*) suggested that a gas chromatographic column in which the partition ratio, k, was varied down the column might exhibit capabilities similar to those offered by programmed temperature gas chromatography. This suggestion has been verified for columns possessing a linear variation in k (*3*). The systematic variation of the partition ratio in an exponential manner has been considered theoretically and experimentally in this work.

In this technique, herein designated exponentially loaded column gas chromatography (ELCGC), the partition ratio is varied continuously (or discontinuously) from the beginning to the end of the column by a continuous (or discontinuous) variation in the liquid loading on each increment of column packing. Columns possessing an exponential gradient in k have been treated theoretically from the viewpoints of solute retention, column efficiency, and resolution. The derived equations have been experimentally verified using a column which closely approximates an exponential gradient—a 25-stage stepwise gradient column.

In ELCGC, column efficiency, for solutes of low or intermediate retention, is comparable to that of a column containing the mean qualtity of stationary phase on the ELCGC column. Of greater importance is the improvement in resolution which is superior for solutes of low or intermediate partition coefficients on the ELCGC column to that on a regular column containing the average liquid loading of the ELCGC column and to that on the linear column containing the same average liquid loading as the exponentially loaded column. The improved resolution results from the combination of the reduced partition ratio and the improved efficiency.

THEORETICAL

Solute Retention Behavior in ELCGC. A list of the symbols employed in this section is presented in the appendix.

Solute retention time, t_r, may be defined by

$$t_r = \int_0^L \frac{dx}{V_s} \tag{1}$$

where V_s is the solute velocity and x is its position down the column of length L. From the fundamental concepts of chromatography, solute velocity is related to the partition ratio, k, by

$$V_s = V_g R_f = \mu(x) R_f = \mu(x)\left(\frac{1}{1+k}\right) \tag{2}$$

For ordinary gas chromatography columns, an expression for retention time can be derived from Equations 1 and 2, as discussed below:

$$t_r = \int_0^L \frac{k+1}{\mu(x)}\,dx = \frac{L}{\bar{\mu}}(1+k) = t_m(1+k) \tag{3}$$

In ELCGC, k is a function of x and thus changes as the solute progresses down the column. Many relationships can be written to describe an x-dependence of k. The case to be considered in this work is an exponential decrease in k with x, as described in Figure 1. For a simple exponential gradient, the partition ratio at any point on the column is

$$k = k_o e^{\alpha x} \tag{4}$$

Thus Equation 2 becomes

$$V_s = V_g R_f = \mu(x) R_f = \mu(x)\left(\frac{1}{1+k_o e^{\alpha x}}\right) \tag{5}$$

The retention time is now

$$t_r = \int_0^L \frac{dx}{V_s} = \int_0^L \left(\frac{1+k_o e^{\alpha x}}{\mu(x)}\right) dx = \int_0^L \frac{dx}{\mu(x)} + k_o \int_0^L \frac{e^{\alpha x}\,dx}{\mu(x)} \tag{6}$$

The first integral in Equation 6 is evaluated by means of the general derivation of the Martin and James compressibility factor as detailed in reference (*4*). The result is

$$\int_0^L \frac{dx}{\mu(x)} = \frac{2L}{3\mu_o}\frac{(a^3-1)}{(a^2-1)} = \frac{L}{\mu_o j} = \frac{L}{\bar{\mu}} = t_m \tag{7}$$

In the course of this derivation, three equations of interest appear. First, carrier gas velocity is related to the pressure drop across the column by

$$\mu = -c\,dP/dx \tag{8}$$

second, from Boyle's law, $P\mu = P_o\mu_o$ = constant. Third, an expression is derived for the solute position down the column, x in terms of c, p and μ:

$$x = L - \frac{c}{2\mu_o P_o}(P^2 - P_o^2) \tag{9}$$

[1] Present address, Queens College, Flushing, N.Y.

(1) E. Alm, R. J. P. Williams, and A. Tiselius, *Acta Chim. Scand.*, **6**, 826 (1952).
(2) H. Purnell, "Gas Chromatography," John Wiley & Sons, Inc., New York, N. Y. 1963, p 388.
(3) D. C. Locke and C. E. Meloan, ANAL. CHEM., **36**, 2234 (1964).
(4) S. Dal Nogare and R. S. Juvet, "Gas–Liquid Chromatography," Interscience Publishers, Inc., New York, N. Y. 1962, p 74.

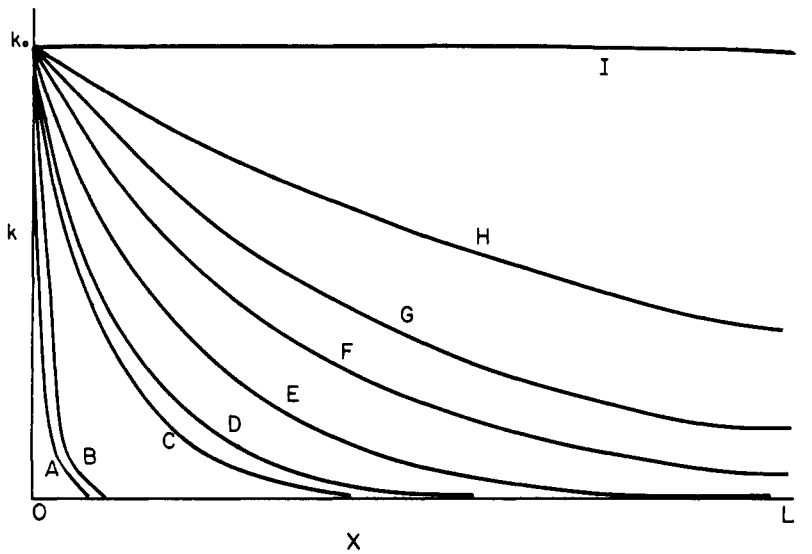

Figure 1. Variation of k with x for various values of α Column (ELCGC)

α equals: A, -1; B, -0.5; C, -0.1; D, -0.08; E, -0.05; F, -0.03; G, -0.02; H, -0.1; I, 0.

Combining these equations in the second integral of equation 6,

$$k_o \int_0^L \frac{e^{\alpha x}dx}{\mu(x)} = \frac{-ck_o e^{\alpha L}e^{\alpha c P_o}}{(\mu_o P_o)^2} \Big/ 2\mu_o \int_{P_i}^{P_o} P^2\, e^{-\alpha c P^2}/2\mu_o P_o dP \tag{10}$$

To make Equation 10 manageable, a Maclaurin's series expansion of e^x is employed:

$$k_o \int_0^L \frac{e^{\alpha x}dx}{\mu(x)} = \frac{-ck_o e^{\alpha L}e^{\alpha c P_o}}{(\mu_o P_o)^2} \Big/ 2\mu_o \times \left[\int_{P_i}^{P_o} P^2 dP - \frac{\alpha c}{2\mu_o P_o}\int_{P_i}^{P_o} 4dP + \left(\frac{\alpha c}{2\mu_o P_o}\right)^2 \int_{P_i}^{P_o} \frac{P^6}{2}dP - \left(\frac{\alpha c}{2\mu_o P_o}\right)^3 \int_{P_i}^{P_o} \frac{P^8}{6} + \ldots\right] \tag{11}$$

The solution of Equation 11 is:

$$k_o \int_0^L \frac{e^{\alpha x}dx}{\mu(x)} = \frac{-ck_o e^{\alpha L}e^{\alpha c P_o}}{(\mu_o P_o)^2} \Big/ 2\mu_o \times \left[\left(\frac{P_i^3 - P_o^3}{3}\right)\frac{-\alpha c}{10\mu_o P_o}(P_i^5 - P_o^5) + \left(\frac{\alpha c}{2\mu_o P_o}\right)^2 \left(\frac{P_i^7 - P_o^7}{14}\right) - \left(\frac{\alpha c}{2\mu_o P_o}\right)^3 \left(\frac{P_i^9 - P_o^9}{54}\right) + \ldots\right] \tag{12}$$

Since the permeability constant, c, in the above equations must be evaluated experimentally, it is convenient to eliminate c from these equations. From Equation 8 and Boyle's law:

$$\mu_o P_o \int_0^x dx = c \int_{P_o}^{P} PdP \tag{13}$$

Integration of Equation 13 and setting $x = L$, $P = P_i$, then c becomes

$$c = \frac{2L\,\mu_o}{P_o\,(\alpha^2 - 1)} \tag{14}$$

Now placing Equation 14 in Equation 12 while recognizing that $P_i/P_o = a$ and rearranging:

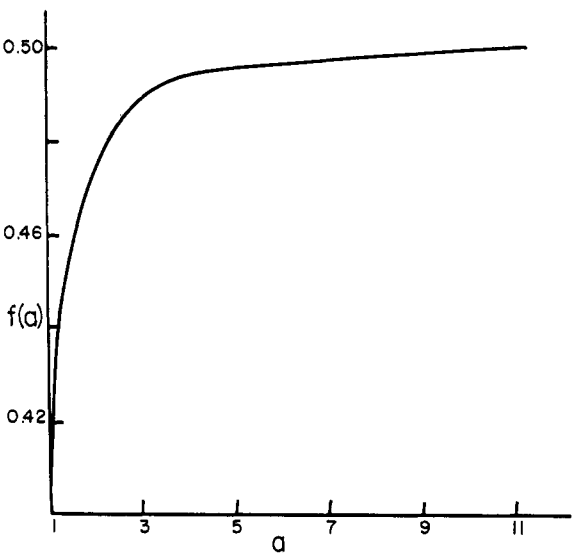

Figure 2. Variation of partition ratio with column pressure drop on ELCGC column

The retention is

$$t_r = t_m + \frac{2Lk_o e^{\alpha L}e^{\alpha L}a^2}{\mu_o(a^2 - 1)} - 1 \times \left[\sum_{n=0}^{\alpha}\left(\frac{-\alpha L}{a^2 - 1}\right)^n \frac{(a^{2n+3} - 1)}{n!\,(2n + 3)}\right] \tag{15}$$

and in terms of $K = (t_r/t_m - 1)$ recognizing that $t_m = \frac{2(a^3 - 1)L}{3(a^2 - 1)\,\mu_o}$

$$K = \frac{3k_o e^{\alpha L}e^{\alpha L/a^2 - 1}}{(a^3 - 1)}\left[\sum_{n=0}^{\alpha}\frac{-\alpha L^n}{a^2 - 1}\frac{(a^{2n+3} - 1)}{n!\,(2n + 3)}\right] \tag{16}$$

Note that when $\alpha = 0$, *i.e.*, when no gradient exists, t_r reduces to its usual form, and $k = k_o$.

In general then, Equation 16 predicts that k is a function of the exponential coefficient, α, the column length, L, the initial k, k_o, and the inlet/outlet pressure ratio, a (or P_i when $P_o = 1$

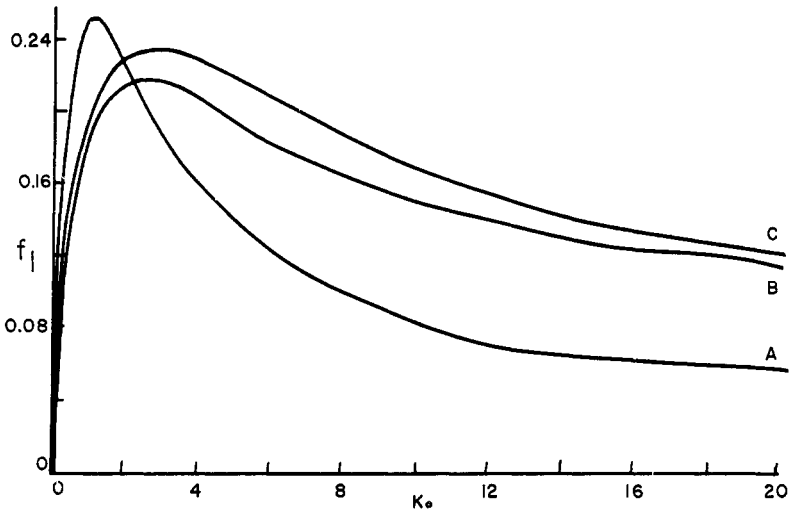

Figure 3. Comparison of dependence of liquid phase mass transfer resistance on partition ratio

$$A.\ \text{Regular column: } fl = \frac{k_o}{(k_o + 1)^2}$$

$$B.\ \text{Linear column: } fl = \frac{\ln (k_o + 1)}{k_o} - \frac{1}{k_o + 1}$$

$$C.\ \text{Exponential column: } fl = \frac{1}{\alpha L}\left[\frac{1}{k_o + 1} - \frac{1}{1 + k_o e^{\alpha L}}\right]$$

atmosphere). For a particular column of given α and L, k is a function only of k_o and a. Figure 2 presents a plot of the coefficient of k_o in Equation 16 as a function of a for a column defined by $\alpha = -0.02$ and $L = 100$ cm.

For ordinary values of a, $f(a)$ increases sharply with increasing inlet to outlet pressure ratio. $f(a)$ asymptotically approaches 0.5 as a becomes large. Equation 16 thus predicts at least a 50% decrease in partition ratio from k_o. In terms of retention time, this corresponds to a minimum decrease given by

$$\Delta t_r = t_m (1 + k_o) - t_m (1 + k_o/2) = \frac{t_m k_o}{2} \qquad (17)$$

This is the same result obtained for the linear gradient system (*3*).

Equation 16 is tedious to use as the summation must be performed over a large number of terms ($n = 10$ to $n = 20$) for ordinary values of a. Thus, some simplification of the partition ratio expression is desirable.

Approximate expressions for t_r and k can be obtained from Equation 6 using the mean value of $\mu(x)$ over the interval $o < x < \mu$. From Equation 6:

$$t_r = \int_0^L \frac{dx}{\mu(x)} + k_o \int_0^L \frac{e^{\alpha x} dx}{\mu(x)} \cong \frac{1}{\bar{\mu}} \int_0^L (1 + k_o e^{\alpha x}) dx \qquad (18)$$

Integration yields:

$$t_r = \frac{1}{\bar{\mu}}\left(L + \frac{k_o e^{\alpha L}}{\alpha} - \frac{k_o}{\alpha}\right) = t_m + \frac{k_o (e^{\alpha L} - 1)}{\alpha \bar{\mu}} \qquad (19)$$

In terms of k,

$$k = t_r/t_m - 1 = k_o \frac{(e^{\alpha L} - 1)}{\alpha L} \qquad (20)$$

For $\alpha = o$, application of L'Hospital's rule reduces Equation 20 to the usual form.

It should be noted that Equations 19 and 20 are constant for a given column and do not predict the pressure dependence of t_r and k.

For purposes of comparison of Equations 16 and 20, the value of α and L ($\alpha = -0.02$ and $L = 100$ cm) employed for Equation 16 in Figure 2 can be used. With this α and L, Equation 20 gives $k = 0.43\, k_o$. For ordinary values of a, this is a satisfactory approximation for most work.

COLUMN EFFICIENCY IN ELCGC

In order to achieve a satisfactory description of plate height in ELCGC, we must recognize that the local plate height, H, will vary with position down the column because of the k-dependency of the mass transfer resistance contributions. In addition, one does not experimentally measure the local plate height, but rather the apparent plate height, $\bar{H}$. These two quantities, H and $\bar{H}$, cannot be equated because of nonuniform conditions (in most cases, of pressure, and in this work, of pressure and k) down the column.

To evaluate column nonuniformity effects on $\bar{H}$, Giddings (*5*) recommends the use of the formula (his Equation 10):

$$\bar{H} = L \frac{\left[\int_0^L \frac{H\, dx}{R_f^2 \mu^2}\right]}{\left[\int_0^L \frac{dx}{R_f \mu}\right]^2} \qquad (21)$$

However, in ELCGC, H, R_f and μ all vary with x which presents a very complicated integral to evaluate. We have thus adopted an approximate procedure similar to that of Locke and Meloan (*3*).

Following the general derivation of the classical (noncoupling) plate height equation such as has been outlined by Dal Nogare and Juvet (*4*), we have

(5) J. C. Giddings, ANAL. CHEM., **34**, 1186 (1962).

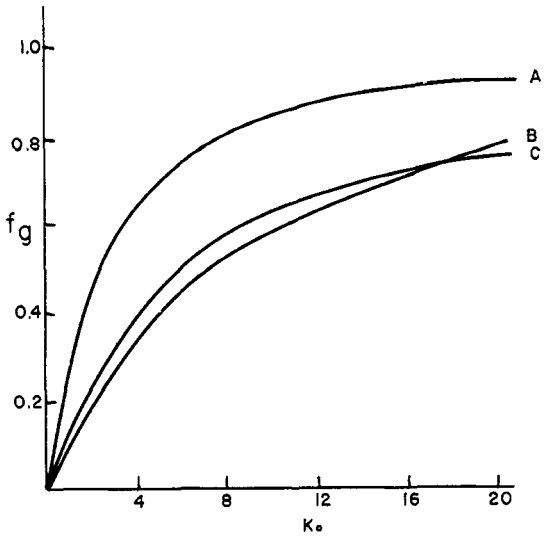

Figure 4. Comparison of dependence of gas phase mass transfer resistance on partition ratio

A. **Regular column:** $f_g = \dfrac{k_o^2}{(k_o + 1)^2}$

B. **Exponential column:** $f_g = \dfrac{1}{\alpha L}\left[\ln\left(\dfrac{1 + k_o e^{\alpha L}}{1 + k_o}\right) + \dfrac{1}{1 + k_o e^{\alpha L}} - \dfrac{1}{1 + k_o}\right]$

C. **Linear column:** $f_g = \dfrac{k_o + 2}{k_o + 1} - \dfrac{2}{k_o}\ln(k_o + 1)$

$$H = A + \frac{B}{\bar{\mu}} + C_l\mu = A + B + \frac{C_l\mu d_l^2}{D_l}\left(\frac{k}{(1 + k)^2}\right) + \frac{C_g\mu d_g^2}{D_2}\left(\frac{k}{(1 + k)^2}\right) \quad (22)$$

The C_g term in this equation is due to Jones (*6*). Later work by Giddings (*5*) and Perrett and Purnell (*7*) has demonstrated the inadequacy of such a k-dependence of the C_g term. They suggest that the gas-phase mass transfer resistance contribution to H is given rather by an equation of the form

$$C_g = \frac{d_p^2}{D_g}\left[0.5 - \frac{0.2}{1 + k} + f(V_l)\right] \quad (23)$$

For the sake of completeness, we will investigate the effect of an exponential gradient loading on both the Jones and the Giddings–Purnell C_g terms.

For the exponential gradient column, C_2, d_g, d_l, $f(V_l)$, and μ all vary with x. To simplify the equations we will use mean values for these parameters, $\bar{d}_g$, $\bar{d}_l$, $C_2 = C_2^1$, and $f^1(v_l)$. We will further assume that velocity gradients in the column are negligible such that $\mu \neq \mu(x)$. Using these approximations and the exponential expression for k, $k = k_o e^{\alpha x}$, in Equation 22 and multiplying through by dx we have

$$Hdx = Adx + Bdx + C_l\mu\bar{d}_l^2\left(\frac{k_o e^{\alpha x}}{(1 + k_o e^{\alpha x})^2}\right)dx + \frac{C_2\mu\bar{d}_g^2}{D_g}\left(\frac{k_o e^{\alpha x}}{1 + k_o e^{\alpha x}}\right) \quad (24)$$

or

$$+ \frac{\mu d_p^2}{D_g}\left[0.5 - \frac{0.2}{1 + k_o e^{\alpha x}} + f^1(V_l)\right]dx \quad (25)$$

where the "or", indicates the alternative expressions for the C_g terms.

(6) W. L. Jones, ANAL. CHEM., **33**, 829 (1961).
(7) R. H. Perrett and H. Purnell, *ibid.*, **35**, 430 (1963).

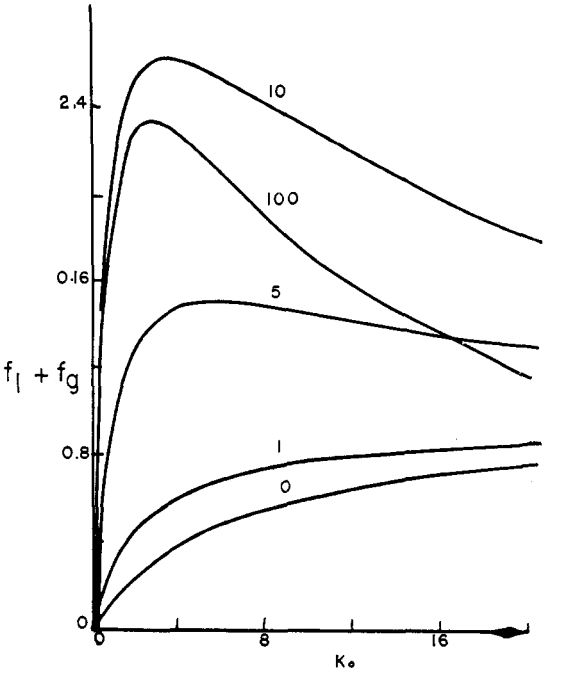

Figure 5. Overall dependence of ELCGC theoretical plate height on partition ratio. Ordinate for r = 100 is $\times 10^{-1}$

Integration of Equations 24 and 25 setting $\alpha = o$, the application of l'Hospital's rule reduces them to the familiar form

$$H = A + \frac{B}{\mu} + \frac{C_l\mu d_l^2}{D_l}\frac{k_o}{(1 + k_o)^2} + \frac{C_2\mu d_g^2}{D_g}\frac{k_o^2}{(1 + k_o)^2} \quad (26)$$

or

$$+ \frac{\mu dp^2}{D_g}\left[0.5 - \frac{0.2}{1 + k_o} + f^1(V_l)\right] \quad (27)$$

Equations 26 and 27 and the corresponding equation of Locke and Meloan (*3*) (their Equation 21) for a linear gradient.

$$H = A + \frac{B}{\mu} + \frac{C_l\bar{d}_l^2}{D_l}\left[\frac{\ln(1 + k_o)}{k_o} - \frac{1}{k_o + 1}\right] + \frac{C_g\mu\bar{d}g^2}{D_g}\left[\frac{k_o + 2}{k_o + 1} - \frac{2}{k_o}\ln(1 + k_o)\right] \text{ or } \frac{\mu dp^2}{D_g} \times 0.5 - \frac{0.2}{k_o}\ln(1 + k_o) + f^1(V_l) \quad (28)$$

are compared graphically in Figures 3 and 4. The ELCGC terms are plotted using column parameters of $\alpha = -0.02$ and $L = 100$ cm. Figure 3 presents the retention dependence of the liquid mass transfer resistance term as a function of k_o. The term of the ELCGC column exhibits a broader maximum at a higher k_o value, but decreases less sharply than either the ordinary column or the linear gradient column. This result is expected for columns with a heavy initial loading, since two phenomena are working against one another. Because of the decreasing amount of liquid from the beginning to the end of the column, the front of a peak is always moving faster than its tail. This results in broader peaks with lower efficiencies. However, the peak is always moving into a region of less significant mass transfer resistance. The first effect predominates for compounds of higher k, while the second effect prevails for compounds of low retention.

Figure 4 depicts the gas-phase mass transfer resistance term as a function of k_o. The curves in Figure 4 indicate that the

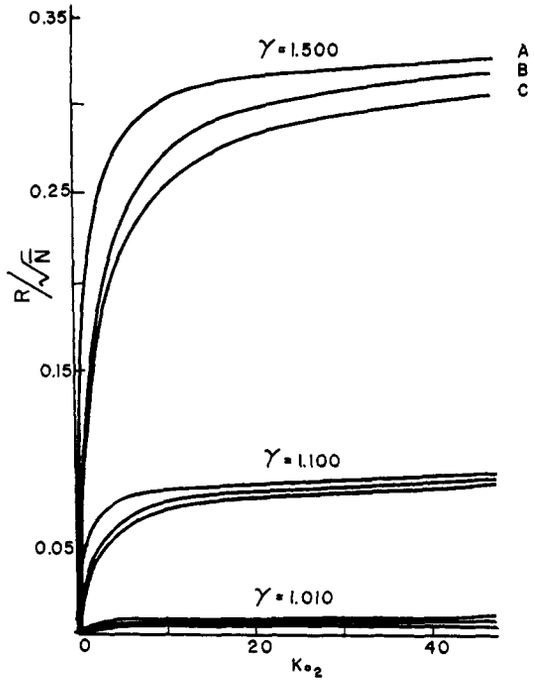

Figure 6. Comparison of resolution on regular, linear, and exponential columns of the same efficiency

A. Regular
B. Exponential
C. Linear

ELCGC column will have less contribution to the plate height from the gas phase term than a regular column with a liquid loading corresponding to k_o. The plate height contribution on the ELCGC column will be less than that for a linear column at low values of k_o, but will be greater than that for a regular column at low values of k_o. The physical significance of these results are not obvious. The curves indicate that an exponential column of overall low liquid loading will be more efficient for all solutes than a regular column corresponding to k_o. Also, for overall low liquid loadings, the exponential column will be more efficient than the linear column of the same k_o for solutes of low retention, and less efficient for solutes of high retention.

Figure 5 presents the overall k_o dependence on plate height in ELCGC for a wide range of liquid loadings. The ordinate for the curve with ratio of liquid to gas mass transfer term coefficients, $r = 100$, is $\pm 10^{-1}$. These curves pass through the same general sequence as the mass transfer terms for regular and for linear columns as the liquid or the gas mass transfer resistance begins to predominate. As r increases—*i.e.*, as the liquid term overpowers the gas term—a maximum appears which shifts to progressively lower k_o values until it stops at $k_o - 2.8$ (at $k_o = 2.2$ for linear and at $k_o = 1$ for regular columns).

The considerations above are ultimately based on the rate equation itself. Giddings' treatment (*8*) is based on the relationship.

$$\bar{H} = \frac{L_\alpha^2}{t_r^2} \tag{29}$$

Equation 21 is readily derived from Equation 29, and is used to generate the f factors, correction factors to account for the discrepancy between the local and the observed plate height.

(8) J. C. Giddings, ANAL. CHEM., **35**, 353 (1963).

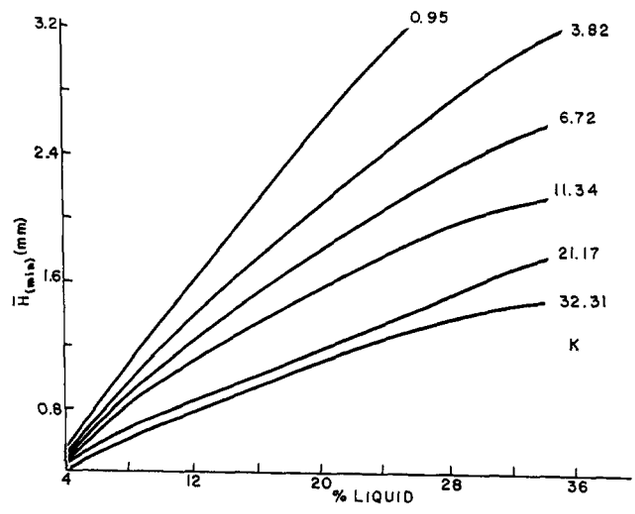

Figure 7. Variation of theoretical plate height with liquid loading

However, the effect of the variation of k down the column on the plate height is not to be considered as a correction since the local plate height changes with position on the column. To obtain an exact description of $\bar{H}$, it would be necessary to use Equation 21 with H, R_f and μ, all functions of x. One can, however, apply approximate corrections for $\bar{H}$ by the use of the f factors in analogy with regular columns. Thus:

$$\bar{H} = A + \left\{\frac{B}{P_o\mu_o} + \frac{C_2\,\bar{d}_g^{\,2}\,P_o\mu_o}{\alpha L D g^o}\left[\ln\left(\frac{1 + k_o e^{\alpha L}}{1 + k_o}\right) + \frac{1}{1 + k_o e^{\alpha L}} - \frac{1}{1 + k_o}\right] \text{ or } + \frac{dp^2 P_o\mu_o}{Dg^o} \times \left[0.3 + \frac{0.2}{\alpha L}\ln\left(\frac{1 + k_o e^{\alpha L}}{1 + k_o}\right) + f^1(V_l)\right]\right\} f_1 + \left\{\frac{C_1\bar{d}_l^{\,2}\,\mu_o}{\alpha L D_L}\left[\frac{1}{1 + k_o} - \frac{1}{1 + k_o e^{\alpha L}}\right]\right\} f_2 \tag{30}$$

RESOLUTION IN ELCGC

The resolution, R, of two peaks of similar retention can be defined by (*9*):

$$R = \frac{t_2 - t_1}{\sigma} \tag{31}$$

where t_1 and t_2 are the retention values of the two peaks. Resolution is 99.9% complete when $R = 6$. For the second (later) peak, the measured mean number of theoretical plates $\bar{N}$, is

$$\bar{N} = \bar{N}_2 = \frac{L}{\bar{H}_2} = 16\left(\frac{t_{r_2}}{w}\right) = \left(\frac{t_2}{\sigma}\right)^2 \tag{32}$$

Average theoretical plate numbers are used since N is a function of x on a gradient column, $\bar{N}$ is used to eliminate the x-dependence of N, which would yield an overly complicated equation to be evaluated.

For gradient column under consideration, t_r, is given by

$$t_r = t_m\,(1 + k_o e^{\alpha x}) \tag{33}$$

Using Equation 32 with the retention time for the second peak,

$$\sigma^2 = t_m\frac{(1 + k_{o2}e^{\alpha x})}{\sqrt{\bar{N}_2}} \tag{34}$$

(9) M. J. Golay, "Gas Chromatography," V. J. Coates *et al.*, Ed., Academic Press, New York, N. Y., 1958, p 315.

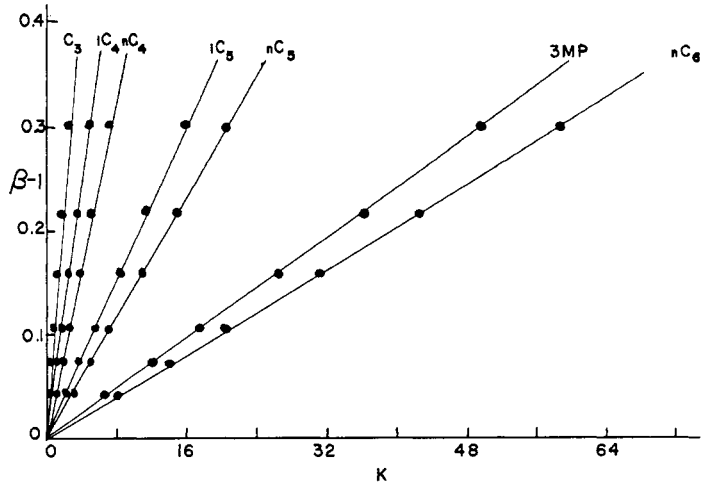

Figure 8. Dependence of partition ratio on β^{-1}

Substitution of Equations 33 and 34 into 31, multiplying by dx, and rearranging, we have

$$\int_0^L R dx = \sqrt{\bar{N}_2}\,(k_{o2} - k_{o1}) \int_0^L \frac{e^{\alpha x}}{1 + k_{o2}e^{\alpha x}}\,dx \qquad (35)$$

Integration of Equation 35 and solution for R gives, letting $\bar{N}_2 = \bar{N}$

$$R = \frac{\sqrt{\bar{N}}}{\alpha L}\left(\frac{\gamma - 1}{\gamma}\right) \ln\left(\frac{1 + k_{o2}e^{\alpha L}}{1 + k_{o2}}\right) \qquad (36)$$

This result is considerably different from the equation for a regular column

$$R = \sqrt{\bar{N}}\left(\frac{\gamma - 1}{\gamma}\right)\left(\frac{k_{o2}}{1 + k_{o2}}\right) \qquad (37)$$

but is somewhat similar to the linear gradient result (*3*), which is

$$R = \sqrt{\bar{N}}\left(\frac{\gamma - 1}{\gamma}\right)\left[\frac{1 - \ln(1 + k_{o2})}{k_{o2}}\right] \qquad (38)$$

However, Equation 36 can be made to resemble Equation 37 by a further rearrangement of Equation 35 which on integrations and solution for R gives

$$R = \sqrt{\bar{N}}\left(\frac{\gamma - 1}{\gamma}\right)\left(\frac{k_{o2}}{\frac{\alpha L}{e^{\alpha L_{-1}}} + k_{o2}}\right) = \sqrt{\bar{N}}\left(\frac{\gamma - 1}{\gamma}\right)\left(\frac{k_{o2}}{C + k_{o2}}\right) \qquad (39)$$

Equation 39 resembles the resolution expression for regular columns (Equation 37). Application of L'Hospital's rule to Equation 36 and to Equation 39 reduces each to Equation 37 for $\alpha = 0$, *i.e.*, when no gradient exists. Equations 36 and 39 are equivalent for given values of α, γ, k_{o2}, L, and $\sqrt{\bar{N}}$. Equation 39 will be employed hereafter, as the calculation of R using Equation 35 is more complicated.

Figure 6 depicts the variation of R with k_{o2} for two peaks of relative retention, γ. In this plot, resolution in ELCGC, which is proportional to

$$\left(\frac{\gamma - 1}{\gamma}\right)\left(\frac{k_{o2}}{\frac{\alpha L}{e^{\alpha L_{-1}}} + k_{o2}}\right) \qquad (40)$$

for a given $\sqrt{\bar{N}}$ constant in Equation 39, is compared with resolution on an ordinary column k_{o2} and the same $\sqrt{\bar{N}}$, which is proportional to

$$\left(\frac{\gamma - 1}{\gamma}\right)\left(\frac{k_{o2}}{1 + k_{o2}}\right) \qquad (41)$$

and the resolution on the linear column of the same k_{o2} and $\sqrt{\bar{N}}$, which is proportional to

$$\left(\frac{\gamma - 1}{\gamma}\right)\left(\frac{1 - \ln(1 + k_{o2})}{k_{o2}}\right) \qquad (42)$$

For the exponential system the column parameters were taken as $\alpha = -0.02$ and $L = 100$ cm.

Figure 6 indicates that resolution on the ELCGC column is intermediate between that of the linear column and that of the regular column . Thus, for two components of relative retention, γ, the ELCGC column requires a larger number of theoretical plates than a regular column, but less plates than a linear column to achieve the same resolution. In general, however, the ELCGC column will provide more efficient operation than either the regular or the linear column, at least for components whose partition ratios are not too large, because, as discussed previously, the components will spend most of their time in regions of progressively lower liquid loadings. The increased efficiency resulting from the decreased liquid loading will, in general, be superior to the decreased efficiency due to the velocity differential between the front and the tail of a peak. Consequently, resolution on the ELCGC column should be superior or equivalent to that on either the regular or the linear column having the same k_{o2} values, provided that these k_{o2} values are not too large.

Finally, Figure 6 demonstrates that as resolution becomes more difficult (as γ decreases to 1.0), the performances of the three columns approach one another for columns of the same efficiency.

EXPERIMENTAL

A Wilken's Aerograph Model A-90-P gas chromatograph with a thermal conductivity detector was used for all measurements. Column and detector temperatures were maintained at 45.0 ± 0.1 °C. The injection port was heated to 120 °C. All measurements were recorded with a Sargent Model SR recorder with a 1 in./min chart speed.

Inlet pressures were measured in torr with a u-shape manometer. Column outlet pressure was always atmospheric. Helium carrier gas flow rates were measured with a soap bubble flow meter.

Phillips Hydrocarbon Blend No. 42 was used in all experiments. Five microliters of vapor was usually sufficient

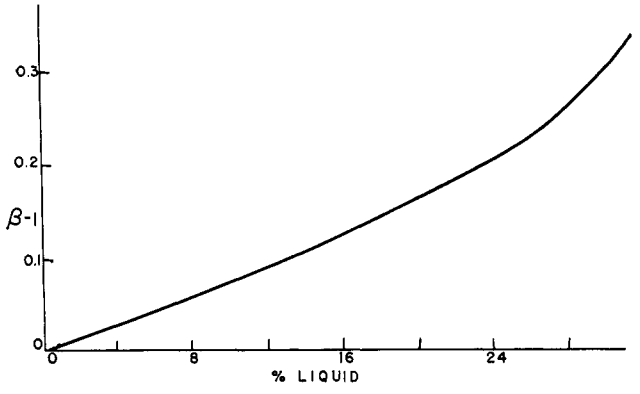

Figure 9. Variation of β^{-1} with liquid loading

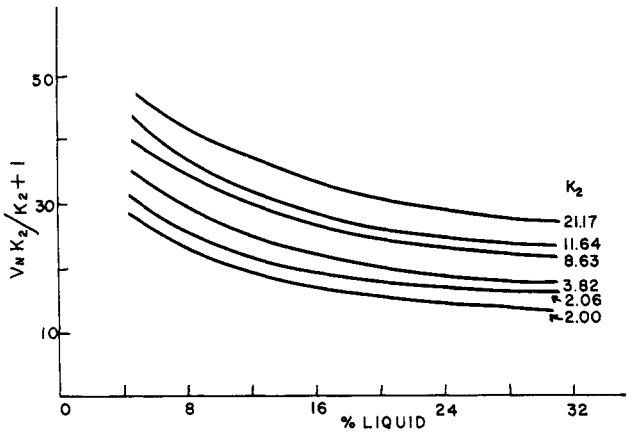

Figure 10. Resolution as a function of liquid loading

sample. The minor components of the blend (total present is 0.23 wt %) are at a nondetectable level. The major components are propane (hereafter abbreviated C_3, comprising 2.2 wt % of the blend), isobutane (iC_4, 8.2%), *n*-butane (nC_4, 20.7%), isopentane (iC_5, 13.0%), *n*-Pentane (nC_5, 15.0%), 3-methyl pentane (3MP, 9.6%), *n*-hexane (nC_6, 12.0%), and *n*-heptane (nC_7, 19.2%). Measurements were made on all detectable components except nC_7.

The columns used in this work (see below) were all prepared from squalane (Eastman No. 7311) and 80/100 mesh Chromosorb P, and were packed by vertical tapping into 0.25-inch o.d. copper tubes. Minimum size glass wool plugs held the packing in place. All columns were conditioned at 45.0 °C for at least 24 hours under a high flow of helium.

Several regular squalane columns were investigated to establish operating conditions and to obtain retention, efficiency, and resolution data for comparison with the ELCGC column. Columns 100 cm long containing 0, 5.0, 10.0, 15.0, 20.0, 25.0, and 30.0 wt. % squalane on 80/100 mesh Chromosorb P were prepared.

Because of the experimental difficulty in preparing a continuous exponential gradient column, the continuous gradient was approximated by a 25-stage stepwise gradient. The column consisted of 4.0 cm of each of the following packings: 30.5, 29.6, 28.5, 27.3, 26.0, 24.8, 23.5, 22.1, 20.7, 19.6, 18.3, 16.9, 15.9, 14.9, 14.0, 13.1, 12.2, 11.3, 10.5, 9.8, 9.3, 8.6, 8.1, 7.2, and 6.9 wt % squalane. The selection of these values is discussed below. Column increment lengths were measured with a 3-mm diameter glass rod which just fits inside a 0.25-inch o.d. tube.

RESULTS AND DISCUSSION

Regular Columns. The regular columns investigated behaved normally, and the results agree well with those reported by Locke and Meloan (*3*, *10*). Since the work of Locke and Meloan contains a thorough report of the results for the regular columns, and since no objection to these results has been raised, the only data to be reported here for regular columns are those which are essential for the investigation of the exponentially loaded column. A plot of $\beta = V_m/V_1$ *vs.* % liquid was similar to that of Dal Nogare and Chiu (*11*), and thus is not reproduced here.

The absence of absorption was verified by plots of partition ratio *vs.* % liquid, which passed through the origin for all compounds studied. The regular and gradient columns gave identical plots of V_g°, the specific retention volume, *vs.* the number of carbon atoms for the normal hydrocarbons.

(10) D. C. Locke, "Studies in Gas Chromatography," Doctoral Dissertation, Kansas State University, Manhattan, Kan., 1964.
(11) S. Dal Nogare and J. Chiu, ANAL. CHEM., **34**, 890 (1962).

Specific retention volume, partition coefficient, *K*, and activity coefficient γ_p, calculated for the various components of the blend on each column all agree satisfactorily with those reported by Locke and Meloan (*3*). Also, plots of H_{min} *vs.* % liquid for various values of *k* are in good agreement with their Figure 11, but are reproduced here as Figure 7 since this plot is necessary for the preparation of Figure 10, as discussed below. Efficiency measurements summarized in a plot of H_{min} *vs. K* were similar to those reported by Dal Nogare and Chiu (*11*), and thus are not reproduced here.

Plots of $\beta^{-1} = V_l/V_m$ as a function of *k* and of β^{-1} as a function of % liquid are presented in Figures 8 and 9, respectively. These agree well with those previously reported (*3*), but are reproduced here because they are necessary for the preparation of the exponentially loaded column, as discussed below.

Finally, Figure 10 presents a plot of $\sqrt{N}k_2/(k_2 + 1)$ as a function of % liquid for several values of k_2. This plot is constructed from data extracted from Figure 7. Figure 10 agrees with Figure 13 of Locke and Meloan (*3*), but is reproduced here as it will be used to determine equivalent liquid loadings on the gradient column.

Gradient Column. The exponentially loaded column was prepared in a 25-stage stepwise approximation of a continuous gradient. A value for an initial liquid loading was arbitrarily chosen (in this case, 31.0%). This was converted to an initial *k*, k_o, through Figures 8 and 9. This k_o was then used with the column parameters, $\alpha = -0.02$ and $L = 100$ cm, in Equation 4 to calculate a *k* value for the midpoint of each *x* increment. The *k* values thus calculated were used with Figures 8 and 9 to obtain the % liquid values necessary to give the desired exponential gradient in *k*. This procedure is required because *k* and % liquid are not directly related. The following weight per cents of squalane were used: 30.5, 29.6, 28.5, 27.3, 26.0, 24.8, 23.5, 22.1, 20.7, 19.6, 18.3, 16.9, 15.9, 14.9, 14.0, 13.1, 12.2, 11.3, 10.5, 9.8, 9.3, 8.6, 8.1, 7.2, and 6.9. The column is diagrammed in Figure 11 where smooth curves are drawn through the midpoints of the *x*-increments. The k_o values for the various compounds are found in Table I.

Theory and experiment are in good agreement for the ELCGC column. Table I demonstrates the prediction of partition ratios using Equation 16. Values of *k* for two pressure drops, *a*, are presented to indicate the prediction of the pressure dependence of *k* on the ELCGC column. Also included in Table I are values of *k* calculated from Equation 20, the approximate expression for *k*. It is seen that Equation 20 gives a reasonable estimate of experimental *k* values for

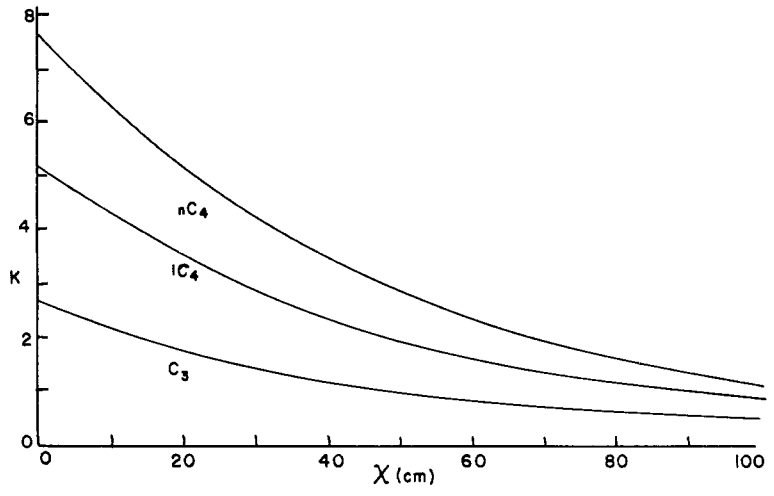

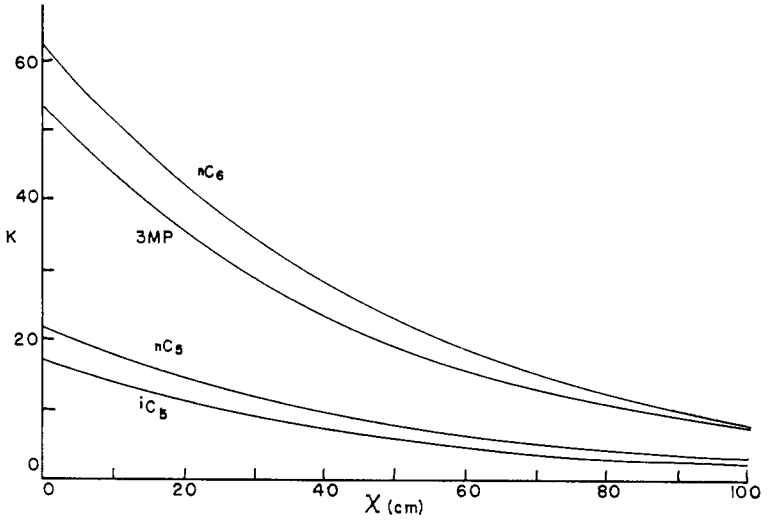

Figure 11. Diagram of exponentially loaded column

A. C_3, iC_4, nC_4
B. iC_5, nC_5, 3MP, nC_6

Table I. Prediction of k on an ELCGC Column

Compd	k_o	k (a = 2.33)		k (a = 2.03)		
		k_{exp}	k_{theor}[a]	k_{exp}	k_{theor}[a]	k_{theor}[b]
C_3	2.59	1.22	1.25	1.21	1.23	1.12
iC_4	5.12	2.53	2.47	2.51	2.43	2.21
nC_4	7.41	3.82	3.57	3.66	3.51	3.20
iC_5	16.9	8.31	8.15	8.11	8.01	7.31
nC_5	21.9	10.9	10.6	10.5	10.4	9.47
3MP	53.8	25.0	25.9	24.8	25.5	23.2
nC_6	62.6	30.2	30.2	29.2	29.7	27.1

[a] From Equation 16.
[b] From Equation 20.

ordinary values of a, but that the values thus obtained are static values, *i.e.*, they do not account for the variation of the partition ratio with the pressure drop. The partition ratios correspond to a regular column with a 19.9% liquid loading for a = 2.33, and to a column with a liquid loading of 19.4% for a = 2.3. The true mean % squalane on the exponential gradient column is 21.6%.

The decreased partition ratio (greater than 50% decrease) is to be desired provided that it is not accompanied by a corresponding loss of efficiency and resolution. Figure 12 depicts the dependence of efficiency on the initial partition ratio. A comparison of Figure 12 with Figure 5 indicates that the exponential gradient column has a ratio of liquid to gas mass transfer resistance coefficients of about 5. This represents a considerable improvement of efficiency over that of a regular column containing an amount of liquid equivalent to the mean % liquid on the ELCGC column. The data are presented in Table II, where equivalent % liquid is the amount of liquid required on a regular column to give the H_{min} (mm) for the particular compound.

Table II. Efficiency on an ELCGC Column

Compound	H_{min} (mm)	Equivalent % liquid
C_3	1.45	12.0
iC_4	1.49	11.9
nC_4	1.38	12.8
iC_5	1.20	16.2
nC_5	1.11	12.4
3MP	1.01	17.0
nC_6	0.74	14.7
		15.0

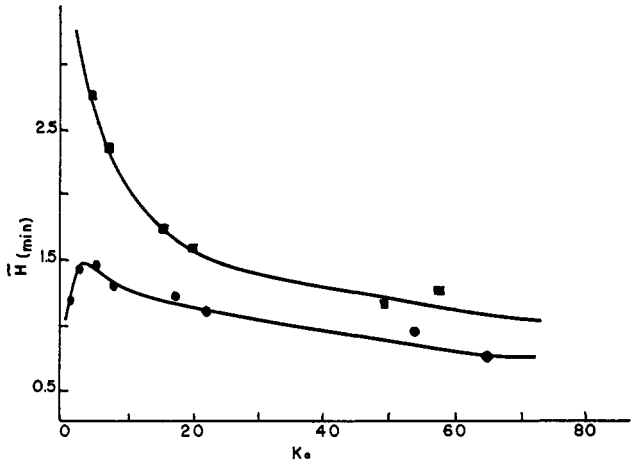

Figure 12. Dependence of ELCGC plate height on initial partition ratio compared with that of a regular 30% column

Top. 30% Squalene (regular)
Bottom. ELCGC

Table III. Equivalent Liquid Loadings on an ELCGC Column

Compd pair	R_{max}	γ	Equivalent % liquid	Equiv. % −21.6%
iC_4–nC_4	6.52	1.447	15.1	−6.5
iC_5–nC_5	6.19	1.295	16.2	−5.4
3MP–nC_6	5.09	1.165	19.2	−2.4

We have now shown, theoretically and experimentally, that the partition ratio on the ELCGC column is reduced by more than 50%, *i.e.*, the retention on an exponentially loaded column with an initial loading of 30.5 wt. % squalane has been reduced to that corresponding to a regular column of less than 20 wt. % squalane (actual value varies with the pressure drop). Further, column efficiency for the exponential gradient column is superior to that for a regular column of 21.6 wt. % squalane, the mean liquid loading of the gradient column.

A comparison of resolutions predicted by Equations 37 and 39 for regular and ELCGC columns, respectively, predicts that for a given $\bar{N}$ and k_{o2}, resolution of the regular column will be superior to that on the ELCGC column. However, we have shown that the ELCGC column is more efficient than a regular column corresponding to the mean % liquid on the gradient column. Thus one would expect better resolution on the ELCGC column than on a regular column of the same mean % liquid, at least for compounds of low and moderate retention.

The three pairs of compounds, iC_4–nC_4, iC_5–nC_5, and 3MP–nC_6, were used to test Equation 39. Figure 13 displays R as a function of μ_o. Agreement with Equation 39 is good. Table III presents the equivalent liquid loadings obtained from Figure 10 and the experimental R and γ values.

On this column, for compounds of $k_{o2} < 44$, resolution is superior to that on a regular 21.6% column. This is presented graphically in Figure 14, a plot of the data in Table III. Comparison of Figure 14 with that for the linear column (*3*) (their Figure 19) indicates the superior resolution available with an exponential gradient.

CONCLUSION

The data of Table III are the ultimate justification for ELCGC. An exponentially loaded column provides better

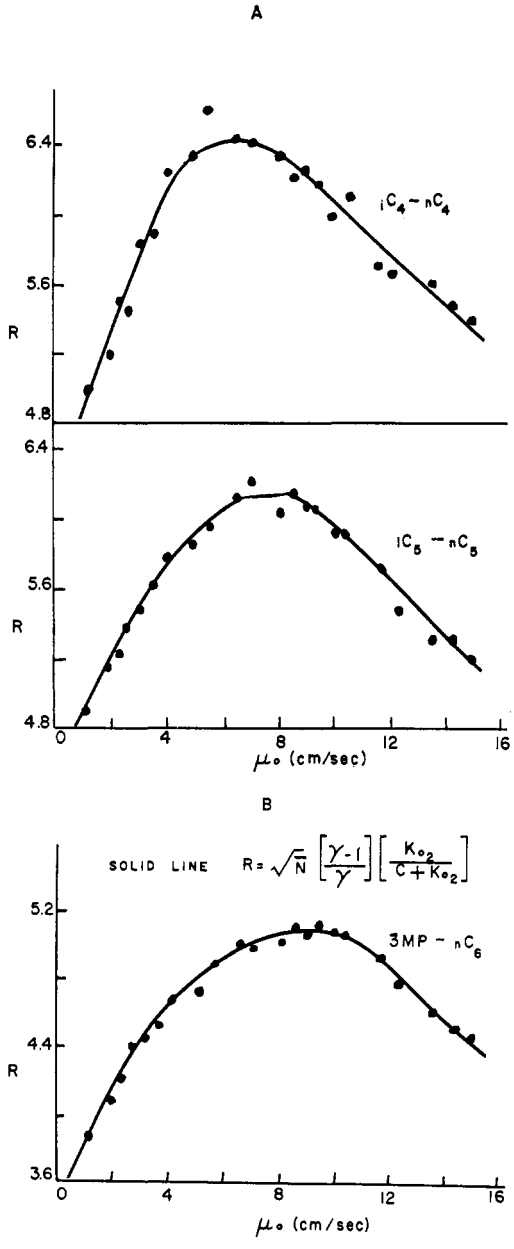

Figure 13. Resolution as a function of V_o for iC_4–nC_4, iC_5–nC_5, and 3MP–nC_6 on the ELCGC Column

A. iC_4–nC_4; iC_5–nC_5
B. 3MP–nC_6

resolution in less time than either regular or linear columns of the same mean liquid loading.

Both resolution and relative velocities increase as the components of a sample move down the column since they continually move into regions of lower liquid loading. For compounds with a large partition ratio, the relative velocity increases faster than the resolution improves. This can be visualized through Equations 16 and 39. Equation 37 predicts that resolution on the regular column will be superior to that on an ELCGC column of the same efficiency. However, the improved efficiency of the ELCGC column over that of corresponding regular or linear columns provides resolution on the exponential column which is superior to that on either the regular or the linear column.

A plot of $\sqrt{\bar{N}}$ *vs.* % liquid shows that the number of theoretical plates decreases approximately linearly only for

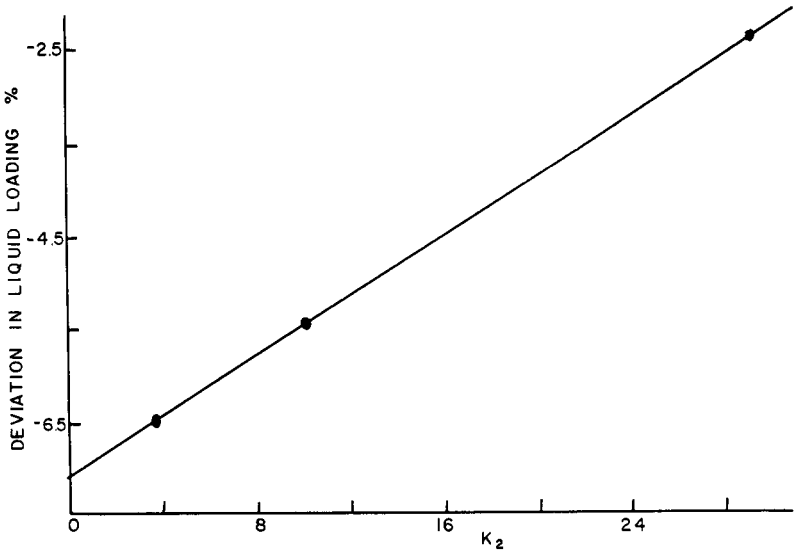

Figure 14. Variation of effective liquid loading with partition ratio on ELCGC column

compounds with large partition ratios, and quite nonlinearly for compounds of low retention, thus justifying the approximation employed in the derivation of Equation 39, that the number of theoretical plates be represented by a mean number, $\bar{N}$. The agreement of experiment with theory, demonstrated in Figure 13, provides the experimental justification for the use of $\bar{N}$.

In addition to providing superior resolution and efficiency in less time than either regular or linear columns of the same average liquid loadings, the ELCGC system also has the advantages claimed for the linear column (*3*); that of being capable of accommodating at least a two-fold increase in sample size and feed volume over that which can be handled on a regular column of $k_o/2$; and that of being more useful than programmed temperature gas chromatography in cases of severe substrate bleeding with increasing temperatures, and with temperature sensitive solutes.

RECEIVED for review December 1, 1966. Resubmitted February 12, 1970. Accepted February 12, 1970. The authors acknowledge the financial assistance provided by the National Defense Education Act.

APPENDIX

List of Symbols Used

Symbol	Definition	Symbol	Definition
A	Term accounting for multipath effect on H, mm	k	Partition ratio
a	Pressure drop on column P_i/P_o	K_i	Peak number in order of elution
B	Term accounting for molecular diffusion in the gas phase, sec^{-1}	k_o	k at column inlet
c	Permeability constant, cm/sec	L	Column length, cm
c_1, c_2, c_2'	Constants	N	Number of theoretical plates in column
C_g	Term accounting for resistance to mass transfer in gas phase, sec	$\bar{N}$	Average N over column.
C_l	Term accounting for resistance to mass transfer in liquid phase, sec.	P	Pressure, torr.
D_g	Diffusion coefficient of solute vapor in carrier gas, cm^2/sec	P_i	Column inlet pressure, torr
D_l	Diffusion coefficient of solute in liquid phase, cm^2/sec	P_o	Column outlet pressure, torr
d_g	Gas film thickness, cm	R	Resolution in number of standard deviations
d_l	Liquid film thickness, cm	r	Ratio of liquid to gas mass transfer resistance coefficients
d_p	Average solid support particle diameter, cm	R_f	Ratio of solute to carrier gas velocities
e	Base of natural logarithm	t_m	Retention value for unsorbed component
f_1	$9(a^4 - 1)(a^2 - 1)/8(a^3 - 1)$	t_r	Retention value for solute
f_2	$J = 3(a^2 - 1)/2(a^3 - 1)$	V_l	Volume of liquid phase in column, cc
$f(V_1)$	Liquid phase maldistribution function	V_M	Volume of mobile phase in column, cc
H	High equivalent to a theoretical plate, mm	v_g	Carrier gas velocity cm/sec
$\bar{H}$	Average H over column, mm	v_s	Solute velocity, cm/sec
$\bar{H}_{min}$	Minimum value of $\bar{H}$, mm	x	Position on the column, cm
j	Gas compressibility correction factor, $3(a^2 - 1)/2(a^3 - 1)$	α	Exponential coefficient, cm^{-1}
K	Partition coefficient	β	Column characteristic, V_M/V_l
		γ	Relative retention, k_2/k_1
		γ_p	Activity coefficient
		ω	Base line width between the extrapolated tangents to the points on inflection of a peak, cm
		σ	Standard deviation